arXiv:1210.4358v1 [cond-mat.mtrl-sci] 16 Oct 2012

A stable all-nitrogen metallic salt at terapascal pressures

Jian Sun [*], [†], **Miguel Martinez-Canales** [‡], **Dennis D. Klug** [§], **Chris J. Pickard** [‡], **Richard J. Needs** [†]

[*] Lehrstuhl für Theoretische Chemie, Ruhr–Universität Bochum, 44780 Bochum, Germany,[†] Theory of Condensed Matter Group, Cavendish Laboratory, J J Thomson Avenue, Cambridge CB3 0HE, United Kingdom,[‡] Department of Physics and Astronomy, University College London, Gower Street, London WC1E 6BT, United Kingdom, and [§] Steacie Institute for Molecular Sciences, National Research Council of Canada, Ottawa, K1A 0R6, Canada

Submitted to Proceedings of the National Academy of Sciences of the United States of America

Nitrogen, as the seventh most abundant element in the universe, is an important constituent of the atmospheres and interiors of planets such as the Earth and the surfaces of moons such as Triton. The phase diagram and equation of state of dense nitrogen is therefore of interest in understanding the fundamental physics and chemistry of planetary processes and in discovering new materials. We predict stable phases of nitrogen at multi-TPa pressures, including a $P4/nbm$ structure consisting of partially charged N$_2^{\delta+}$ pairs and N$_5^{\delta-}$ tetrahedra, which is stable in the range 2.5–7.1 TPa. This is followed by a modulated $Fdd2$ structure at 7.1–11.5 TPa, which also exhibits significant charge transfer. The $P4/nbm$ metallic nitrogen salt and $Fdd2$ modulated structure exhibit strongly ionic features and charge density distortions, which is unexpected in an element at such high pressures and could represent a new class of nitrogen materials.

New materials under extreme conditions | Density functional theory | *ab initio* | Crystal structure predictions | polymerization of molecular solids

The polymerization of molecular nitrogen under pressure has been very actively researched over the past two decades and has stimulated many experimental [1, 2, 3, 4, 5, 6, 7, 8, 9] and theoretical [10, 11, 12, 13, 14, 15, 16, 17, 18, 19, 20, 21, 22, 23, 24, 25, 26, 27] investigations. Density functional theory (DFT) studies suggested that dissociation of nitrogen could occur at high pressures which were, nevertheless, attainable in diamond anvil cell (DAC) experiments. In a ground-breaking paper, Mailhiot *et al.* [13] predicted polymerization of nitrogen molecules under pressure, leading to the formation of the "cubic gauche" framework structure. After considerable efforts [1, 2], cubic gauche nitrogen was finally synthesized by Eremets *et al.* [5], a decade after its prediction. The polymeric phase is quench recoverable to ambient conditions, where it exists as a rather unstable high-energy-density material (HEDM) [5]. Under ambient conditions an energy of roughly 1.5 eV/atom ($\approx$ 10330 J/g) is released on converting cubic gauche nitrogen to molecular N$_2$, which is more than twice the energy density of TNT (about 4686 J/g). Polymeric nitrogen [5], or high–N content salts [28], are therefore expected to be excellent candidates as high-energy-density materials.

The N$\equiv$N triple bond is one of the strongest known and breaking it requires surmounting a substantial energetic barrier. However, at high temperatures the triple bond breaks at pressures above about 110 GPa [5], a much lower pressure than predicted for the single bond in H$_2$ [29] and the double bond in O$_2$, which is predicted to survive up to 2 TPa [30, 31]. Once the N$\equiv$N triple bond is broken, a wide variety of structures can be adopted, similar to phosphorus and arsenic, and many studies aimed at elucidating the phase diagram of nitrogen have been published.

The set of candidate structures includes simple cubic, the isoelectronic "black phosphorus" and α-arsenic or cis-trans and $Cmcm$ chain structures, etc. [10, 13, 11, 12, 15, 16, 16, 17, 18, 24] Nevertheless, only the "black phosphorus" structure seemed feasible, as it was predicted to become more stable than cubic gauche above $\sim$210 GPa [13, 16, 22]. The advent of structure searching using DFT methods marked a significant advance; under conditions in which standard chemical intuition may no longer be reliable, new stable polymeric nitrogen phases beyond cubic gauche have been proposed, including the layered $Pba2$ and framework $P2_12_12_1$ structures [26, 25]. "Black phosphorus" was subsequently ruled out on energetic grounds. These phases have in common a large DFT band gap that hardly closes with pressure. Nitrogen compounds could form metallic phases at high pressures and/or temperatures, which could have important consequences for understanding planetary processes.

Large compressions normally lead to an increase in the atomic coordination numbers and metallization, as predicted in, for example, hydrogen [29, 32], carbon [33, 34], and oxygen [30], as well as observed in many other systems. [35] The coordination number of the atoms in solid nitrogen increases from one to three on transformation from the molecular to cubic gauche forms and three-fold coordination persists in higher pressure structures.

All high-pressure nitrogen structures proposed so far are insulating. Although an increase in coordination number with pressure is physically reasonable, it is by no means universal. For example, aluminum transforms into more open structures at TPa pressures as the valence electrons move away from the ions in the formation of "electride structures" [36] although, as must occur in a pressure-induced equilibrium phase transition, the density increases at the transition, and well-packed structures are strongly disfavored in oxygen up to at least 25 TPa [30]. The coordination number of nitrogen has not been determined at pressures above 400 GPa, and a metallic phase of nitrogen has not yet been reported.

Materials under TPa pressures are important in planetary science, for example, the pressure at the center of Jupiter is estimated to be about 7 TPa [37]. Dynamical shock wave [37, 38, 39] and ramped compression experiments [40, 41] are increasingly being used to investigate materials at TPa pressures. Even more extreme conditions are attainable in laser ignition experiments [42]. Experimental determinations of structures are not, however, currently possible at TPa pressures and therefore theoretical predictions are particularly important. [33, 32, 36, 34, 30] In this work we focus on the structural phases of nitrogen at multi-TPa pressures.

Results

Crystal structures and charge transfer. We have used *ab initio* random structure searching (AIRSS) [43, 44] and DFT methods to find candidate structures of nitrogen up to multi-TPa pressures. These searches have enabled us to identify novel candidate nitrogen structures that are more stable than previously known ones. Four of them are thermodynamically stable within certain pressure ranges, namely,

---

Reserved for Publication Footnotes

$P4/nbm$ (Z=14), $Fdd2$ (Z=48), $R\bar{3}m$ (Z=1) and $I4_1/amd$ (Z=4). Most interestingly, the tetragonal $P4/nbm$ structure is characterized by the presence of N_2 pairs and N_5 tetrahedra, while the orthorhombic $Fdd2$ structure is modulated, as depicted in Fig. 1(a) and (b).

At 2.5 TPa, the N-N bond length within the N_5 tetrahedra of $P4/nbm$ is 1.13 A, and the shortest distance between the corners of the tetrahedra and N_2 dimers is 1.26 A. The N-N bond length within the dimer of about 1.17 A is significantly shorter than the N-N separation between adjacent dimers (about 1.29 A), which implies that the dimers are well separated.

The unique structure of the $P4/nbm$ phase led us to investigate the charges on the different atomic sites. We used the wavefunction-based Mulliken population and charge-density based Bader [45] methods to analyze the charge transfer. As summarized in Table 1, the two methods lead to the same conclusions; the N_5 tetrahedra are negatively charged and serve as anions while the N_2 dimers are positively charged and act as cations, and thus the $P4/nbm$ structure resembles an all-nitrogen salt. The resultant charges (about $\pm 0.22e$ from Mulliken analysis and about $\pm 0.37e$ from Bader analysis) are substantial, although they depend somewhat on the definition of the atomic charges.

The complicated $Fdd2$ structure has a 48-atoms conventional cell, and the atoms are arranged in undulating layers, as depicted in Fig. 1(b). The charge distribution of $Fdd2$ also exhibits large distortions. As shown in Fig. 1(b) and Table 1, although all the atoms are at 16b sites, each orbit has a different character: there is a group of strong electron acceptors (Bader charge Q_B=-0.36e, red), a group of strong electron donors (Q_B=0.38e, blue), and a group of nearly neutral atoms (Q_B=-0.02e, green). Due to the undulation, with the inequivalent z positions averaging at 0.1254, the $Fdd2$ structure is very similar to a charge density wave (CDW) modulation. The appearance of strong charge transfer effects in an element at such high pressures is most unexpected, as the resulting Coulomb energy is substantial.

We also found a layered $Cmca$ structure similar to "black phosphorus", which becomes thermodynamically stable at about 2 TPa. As depicted in the supplementary information, the $Cmca$ structure consists of three-fold-coordinated nitrogen atoms and has zig-zag layers, with a shortest N-N distance of about 1.15 A at 2.5 TPa, which is much shorter than the N-N separation between the layers of about 1.56 A. Layered structures also appear in the high-pressure phases of other small molecules of first row atoms, e.g., CO [46] and CO_2 [47]. The nitrogen atoms in the $R\bar{3}m$ structure are six-fold-coordinated and form distorted octahedra. Pure four-fold coordinated structures often appear in our searches at 3 TPa, but they are less favorable than $Cmca$ and $P4/nbm$. The crystal structures and charge transfers of the newly predicted stable phases are summarized in Table 1.

Energetics. As can be seen in the enthalpy-pressure relations of Fig. 2(a), solid nitrogen undergoes a series of structural phase transitions beyond the previously-known framework $P2_12_12_1$ polymeric phase [25, 26] and recently discovered diamondoid structure ($I\bar{4}3m$) [27]: $I\bar{4}3m \xrightarrow{2.1\text{ TPa}} Cmca \xrightarrow{2.5\text{ TPa}} P4/nbm \xrightarrow{7.1\text{ TPa}} Fdd2 \xrightarrow{11.5\text{ TPa}} R\bar{3}m \xrightarrow{30\text{ TPa}} I4_1/amd$. This partially ionic $P4/nbm$ phase is stable over a wide pressure range, but compression to about 7.1 TPa leads to the modulated $Fdd2$ structure. The $Fdd2$ structure is the most favorable phase from about 7.1–11.5 TPa, whereupon it transforms into a six-fold-coordinated hexagonal $R\bar{3}m$ phase. As shown in the inset in Fig. 2, nitrogen forms a $P4_1/amd$ structure similar to Cs-IV [48] at about 30 TPa.

The volume-pressure relations of the most stable phases are shown in Fig. 2(b). The volume decreases by about 2.5% at the transition from $I\bar{4}3m$ to $Cmca$ at 2.1 TPa, 0.7% at the transition from $Cmca$ to $P4/nbm$ at 2.5 TPa, 0.6% at the transition from $P4/nbm$ to $Fdd2$ at 7.1 TPa, and 0.5% at the $Fdd2$ to $R\bar{3}m$ transition at 11.5 TPa.

Electronic structures. The electronic band structures and projected densities of states (PDOS) of $Cmca$ at 2.0 TPa, $P4/nbm$ at 3.0 TPa, and $Fdd2$ at 8.0 TPa, are shown in Fig. 3, decomposed into s and p components. The $P2_12_12_1$ and $I\bar{4}3m$ structures are semiconducting at 2.5 TPa, but the band structures of $Cmca$, $P4/nbm$, and $Fdd2$ shown in Fig. 3 and $R\bar{3}m$ are metallic, see the supplementary material. The insulating state of nitrogen persists to about 2.0 TPa, which is considerably higher than in other light elements such as hydrogen, carbon and oxygen. [30]

The band structure of $Cmca$ at 2.0 TPa features a partially filled Dirac cone between the Y and Γ points, similar to the one that appears in electron doped graphene. [49] The projected density of states in these metallic structures arises from the s and p orbitals which extend over essentially the same energy interval, with both s and p orbitals contributing to the electronic density of states at the Fermi level and conduction bands, which indicates strong sp hybridization in the $Cmca$, $P4/nbm$ and $Fdd2$ structures. The densities of states at the Fermi levels of $P4/nbm$ and $Fdd2$ are higher than in $Cmca$, implying that $Cmca$ is less metallic.

Discussion

The dynamical stability of the newly predicted stable structures was investigated by calculating their phonon dispersion relations. As shown in Fig. 4 and in the supplementary material, all of the structures are predicted to be mechanically and dynamically stable at the specified pressures. The phonon dispersion relation of $P4/nbm$ shows steep acoustic branches together with fairly flat optical modes. This supports the view that $P4/nbm$ is formed of atomic units: the N–N vibrons as well as the breathing mode of the tetrahedra are essentially dispersionless, and well screened by the electronic cloud.

On the other hand, the phonon mode of $Fdd2$ corresponding to the amplitude variation of the undulating layers drops to a very low frequency of about 190 cm^{-1}. For comparison, the next lowest-lying mode (the relative sliding mode) has a much higher frequency of about 1300 cm^{-1}, because the shear mode brings atoms of the same charge closer together.

The formation of N_2 pairs and N_5 tetrahedra in $P4/nbm$ was deduced from the calculated bond lengths and confirmed by the charge density plot in Fig. 5(b), where the atoms between the tetrahedron center and corners, and between the two atoms within the dimers, form strong covalent bonds. The electron localization function (ELF) shown in the supplementary material provides additional evidence for the formation of tetrahedra and dimers in $P4/nbm$.

The formation of charged units from an elementary compound has also been observed in γ–Boron [50]. The pressures of interest in the present study are much larger than those at which γ–Boron has been observed and, besides, $P4/nbm$–nitrogen is a very different system. The charge transfer in boron satisfies its tendency to form electron deficient icosahedra. Based on the structural richness of phosphorus and arsenic one might assume that nitrogen could form similarly rich bonding patterns once the triple bond is broken. At 2 TPa, however, packing efficiency is crucial and one would expect structures with high coordination numbers to be formed. For example, the coordination number of $Cmca$ is 3, compared with 6 in the $R\bar{3}m$ phase. It is therefore reasonable to expect that the average coordination of nitrogen in the $P4/nbm$ and $Fdd2$ structures would be between 3 to 6. In $P4/nbm$, if one employs a longer bond criterion, e.g., 1.30 A, the coordination number for the corners of the tetrahedra, their centers and the nitrogen atoms in the chains are 3, 4, and 6, respectively, as shown in Fig. S5 of the supplementary information. In this metallic phase the variation in coordination (or the inhomogeneity of the density of ions) leads to charge transfer from the highly-coordinated atoms ("N_2 pairs") to the lower coordinated ones ("tetrahedra" corners). This charge transfer allows the $P4/nbm$ structure to form a unique metallic all-nitrogen salt. Each atom in the 1D chains perpendicular to the tetrahedra layers has four long bonds to the corners of the tetrahedra, thus only one electron is left. The 1D chain with uniform N–N distances is unstable and undergoes a Peierls distortion, similar to that in lithium [51], and N_2 pairs are formed.

Although $Fdd2$ also shows clear variation in coordination and charge transfer, the atomic arrangement is completely different from that in $P4/nbm$. This phase has undulating layers, formed from distorted parallelepipeds, resembling a CDW. CDWs have been observed previously in chalcogenides under pressure [52]. In light of the charge transfer, the buckling of layers could be viewed not only as a symmetry breaking, but also as allowing the positive and negative ions to approach one another and reduce the energy. In addition, the charge transfer might create atomic sites similar to those in carbon at comparable pressures, although the $Fdd2$ bandstructure shows very different behaviour [34]. While carbon expels charge from the $2s$ levels at high compression, eventually forming an electride, the bottom of the $Fdd2$ valence band shows a large $2s$ population. Charge depletion from the $2s$ levels will only arise with the transition to the superconducting $R\bar{3}m$ phase, at almost 12 TPa. Electride structures are found for example in carbon [34] and aluminum [36] at very high pressures, but they do not to appear in nitrogen up to at least 100 TPa. While intuition suggests that close-packed structures should be favored under extreme pressures, this is not the case for nitrogen even at 100 TPa where, for example, the fcc structure is almost 2 eV per atom higher in enthalpy than $I4_1/amd$.

Methods

Structure search. The *ab initio* random structure searching (AIRSS) method [43, 44] was used to identify low-enthalpy structures of nitrogen at multi-TPa pressures. Extensive searches were performed at selected combinations of 2, 3, 4, 5, 6, 7, 8, 9, 10, 11, 12, 13, 14, 15, 16, 17, 18, 19, 20, 21, 22, 24 nitrogen atoms per cell at 1, 2, 3, 4, 5, 7, 10, 15, 20, 50 and 100 TPa. More than 47,000 structures in total were optimized using DFT. Additional searches were performed using initial structures consisting of random packings of N_2 dimers and N_5 tetrahedra, in order to study the partially-ionic structures in more detail. No better structure than $P4/nbm$ was found.

***Ab initio* calculations.** We used the CASTEP plane-wave DFT code [53] and an ultrasoft pseudopotential generated with a small core radius to avoid overlapping of the core radii at the high-pressures studied. The enthalpy-pressure relations of the structures were recalculated using very hard Projector Augmented Wave (PAW) pseudopotentials and the VASP code [54] with a plane-wave basis set cutoff energy of 1000 eV. Phonon and electron-phonon coupling calculations were performed using DFT perturbation theory [55] with the ABINIT [56] and Quantum ESPRESSO codes [57]. Very high cutoff energies (1632 eV for ABINIT and 952 eV for Quantum ESPRESSO), together with large numbers of k-points, were used to obtain convergence of the enthalpy differences between phases to better than 5×10^{-3} eV per atom. Calculations were performed with the different codes to cross-check the transition pressures.

ACKNOWLEDGMENTS.

J.S. gratefully acknowledges financial support from the Alexander von Humboldt (AvH) foundation and Marie Curie actions. M.M.C. C.J.P. and R.J.N. were supported by the EPSRC. The calculations were carried out at BOVILAB@RUB (Bochum), LIDOng (Dortmund), on the supercomputers at NRC (Ottawa) and UCL (London).

References

1. Goncharov AF, Gregoryanz E, Mao HK, Liu ZX, Hemley RJ (2000), Optical evidence for a nonmolecular phase of nitrogen above 150 GPa *Phys Rev Lett* 85:1262–1265.
2. Eremets ML, Hemley RJ, Mao H, Gregoryanz E (2001), Semiconducting non-molecular nitrogen up to 240 GPa and its low-pressure stability *Nature* 411:170–174.
3. Gregoryanz E, Goncharov AF, Hemley RJ, Mao HK (2001), High-pressure amorphous nitrogen *Phys Rev B* 64:052103.
4. Gregoryanz E, Goncharov AF, Hemley RJ, Mao HK, Somayazulu M, Shen GY (2002), Raman, infrared, and x-ray evidence for new phases of nitrogen at high pressures and temperatures *Phys Rev B* 66:224108.
5. Eremets MI, Gavriliuk AG, Trojan IA, Dzivenko DA, Boehler R (2004), Single-bonded cubic form of nitrogen *Nature Mater* 3:558–563.
6. Eremets MI, Gavriliuk AG, Serebryanaya NR, Trojan IA, Dzivenko DA, Boehler R, Mao HK, Hemley RJ (2004), Structural transformation of molecular nitrogen to a single-bonded atomic state at high pressures *J Chem Phys* 121:11296–11300.
7. Eremets MI, Gavriliuk AG, Trojan IA (2007), Single-crystalline polymeric nitrogen *Appl Phys Lett* 90:171904.
8. Gregoryanz E, Goncharov AF, Sanloup C, Somayazulu M, Mao HK, Hemley RJ (2007), High P-T transformations of nitrogen to 170 GPa *J Chem Phys* 126:184505.
9. Lipp MJ, Klepeis JP, Baer BJ, Cynn H, Evans WJ, Iota V, Yoo CS (2007), Transformation of molecular nitrogen to nonmolecular phases at megabar pressures by direct laser heating *Phys Rev B* 76:014113.
10. McMahan AK, Lesar R (1985), Pressure Dissociation Of Solid Nitrogen Under 1 Mbar *Phys Rev Lett* 54:1929–1932.
11. Martin RM, Needs RJ (1986), Theoretical-Study Of The Molecular-To-Nonmolecular Transformation Of Nitrogen At High-Pressures *Phys Rev B* 34:5082–5092.
12. Lewis SP, Cohen ML (1992), High-Pressure Atomic Phases Of Solid Nitrogen *Phys Rev B* 46:11117–11120.
13. Mailhiot C, Yang LH, McMahan AK (1992), Polymeric Nitrogen *Phys Rev B* 46:14419–14435.
14. Mitas L, Martin RM (1994), Quantum Monte-Carlo Of Nitrogen - Atom, Dimer, Atomic, And Molecular-Solids *Phys Rev Lett* 72:2438–2441.
15. Alemany MMG, Martins JL (2003), Density-functional study of nonmolecular phases of nitrogen: Metastable phase at low pressure *Phys Rev B* 68:024110.
16. Mattson WD, Sanchez-Portal D, Chiesa S, Martin RM (2004), Prediction of new phases of nitrogen at high pressure from first-principles simulations *Phys Rev Lett* 93:125501.
17. Zahariev F, Hu A, Hooper J, Zhang F, Woo T (2005), Layered single-bonded nonmolecular phase of nitrogen from first-principles simulation *Phys Rev B* 72:214108.
18. Oganov AR, Glass CW, Ono S (2006), High-pressure phases of $CaCO_3$: Crystal structure prediction and experiment *Earth Planet Sci Lett* 241:95–103.
19. Uddin J, Barone V, Scuseria GE (2006), Energy storage capacity of polymeric nitrogen *Molec Phys* 104:745–749.
20. Zahariev F, Dudiy SV, Hooper J, Zhang F, Woo TK (2006), Systematic method to new phases of polymeric nitrogen under high pressure *Phys Rev Lett* 97:155503.
21. Caracas R, Hemley RJ (2007), New structures of dense nitrogen: Pathways to the polymeric phase *Chem Phys Lett* 442:65–70.
22. Wang XL, He Z, Ma YM, Cui T, Liu ZM, Liu BB, Li JF, Zou GT (2007), Prediction of a new layered phase of nitrogen from first-principles simulations *J Phys: Condens Matter* 19:425226.
23. Zahariev F, Hooper J, Alavi S, Zhang F, Woo TK (2007), Low-pressure metastable phase of single-bonded polymeric nitrogen from a helical structure motif and first-principles calculations *Phys Rev B* 75:140101.
24. Yao YS, Tse JS, Song Z, Klug DD, Sun J, Le Page Y (2008), Structures and superconducting properties of the high-pressure IV and V phases of calcium from first principles *Phys Rev B* 78:054506.
25. Pickard CJ, Needs RJ (2009), High-Pressure Phases of Nitrogen *Phys Rev Lett* 102:125702.

26. Ma YM, Oganov AR, Li ZW, Xie Y, Kotakoski J (2009), Novel High Pressure Structures of Polymeric Nitrogen *Phys Rev Lett* 102:065501.
27. Wang X, Wang Y, Miao M, Zhong X, Lv J, Li J, Chen L, Pickard CJ, Ma Y (2012), Diamondoid Structure of Polymeric Nitrogen at High Pressures, arXiv:1206.5668 [cond-mat.mtrl-sci].
28. Haiges R, Schneider S, Schroer T, Christe K (2004), High-energy-density materials: Synthesis and characterization of $N_5^+P(N_3)_6^-$, $N_5^+B(N_3)_4^-$, $N_5^+HF_2^-$·nHF, $N_5^+BF_4^-$, $N_5^+PF_6^-$, and $N_5^+SO_3F^-$ *Angew Chem Int Ed* 43:4919–4924.
29. Pickard CJ, Needs RJ (2007), Structure of phase III of solid hydrogen *Nature Phys* 3:473–476.
30. Sun J, Martinez-Canales M, Klug DD, Pickard CJ, Needs RJ (2012), Persistence and Eventual Demise of Oxygen Molecules at Terapascal Pressures *Phys Rev Lett* 108:045503.
31. Zhu L, Wang Z, Wang Y, Zou G, Mao Hk, Ma Y (2012), Spiral chain O_4 form of dense oxygen *Proc Natl Acad Sci USA* 109:751–753.
32. McMahon JM, Ceperley DM (2011), Ground-State Structures of Atomic Metallic Hydrogen *Phys Rev Lett* 106:165302.
33. Sun J, Klug DD, Martonak R (2009), Structural transformations in carbon under extreme pressure: Beyond diamond *J Chem Phys* 130:194512.
34. Martinez-Canales M, Pickard CJ, Needs RJ (2012), Thermodynamically Stable Phases of Carbon at Multiterapascal Pressures *Phys Rev Lett* 108:045704.
35. Grochala W, Hoffmann R, Feng J, Ashcroft NW (2007), The Chemical Imagination at Work in Very Tight Places *Angew Chem Int Ed* 38:3620–3642.
36. Pickard CJ, Needs RJ (2010), Aluminium at terapascal pressures *Nature Materials* 9:624–627.
37. Jeanloz R, Celliers PM, Collins GW, Eggert JH, Lee KKM, McWilliams RS, Brygoo S, Loubeyre P (2007), Achieving high-density states through shock-wave loading of precompressed samples *Proc Natl Acad Sci USA* 104:9172–9177.
38. Knudson MD, Desjarlais MP, Dolan DH (2008), Shock-Wave Exploration of the High-Pressure Phases of Carbon *Science* 322:1822–1825.
39. Eggert JH, Hicks DG, Celliers PM, Bradley DK, McWilliams RS, Jeanloz R, Miller JE, Boehly TR, Collins GW (2010), Melting temperature of diamond at ultrahigh pressure *Nature Phys* 6:40–43.
40. Hawreliak J, Colvin J, Eggert J, Kalantar DH, Lorenzana HE, Pollaine S, Rosolankova K, Remington BA, Stolken J, Wark JS (2007), Modeling planetary interiors in laser based experiments using shockless compression *Astrophys Space Sci* 307:285–289.
41. Bradley DK, Eggert JH, Smith RF, Prisbrey ST, Hicks DG, Braun DG, Biener J, Hamza AV, Rudd RE, Collins GW (2009), Diamond at 800 GPa *Phys Rev Lett* 102:075503.
42. Kritcher A, Döppner T, Fortmann C, Ma T, Landen O, Wallace R, Glenzer S (2011), In-Flight Measurements of Capsule Shell Adiabats in Laser-Driven Implosions *Physical Review Letters* 107:015002.
43. Pickard CJ, Needs RJ (2006), High-pressure phases of silane *Phys Rev Lett* 97:045504.
44. Pickard CJ, Needs RJ (2011), Ab initio random structure searching *J Phys: Condens Matter* 23:053201.
45. Bader RFW (1990) *Atoms in Molecules. A Quantum Theory* (Oxford University Press, Oxford).
46. Sun J, Klug DD, Pickard CJ, Needs RJ (2011), Controlling the Bonding and Band Gaps of Solid Carbon Monoxide with Pressure *Phys Rev Lett* 106:145502.
47. Sun J, Klug DD, Martonak R, Montoya JA, Lee MS, Scandolo S, Tosatti E (2009), High-pressure polymeric phases of carbon dioxide *Proc Natl Acad Sci USA* 106:6077–6081.
48. Takemura K, Minomura S, Shimomura O (1982), X-Ray Diffraction Study of Electronic Transitions in Cesium under High Pressure *Phys Rev Lett* 49:1772–1775.
49. Giovannetti G, Khomyakov PA, Brocks G, Karpan VM, van den Brink J, Kelly PJ (2008), Doping Graphene with Metal Contacts *Phys Rev Lett* 101:026803.
50. Oganov AR, Chen JH, Gatti C, Ma YZ, Ma YM, Glass CW, Liu ZX, Yu T, Kurakevych OO, Solozhenko VL (2009), Ionic high-pressure form of elemental boron *Nature* 457:863–867.
51. Neaton JB, Ashcroft NW (1999), Pairing in dense lithium *Nature* 400:141–144.
52. Degtyareva O, Gregoryanz E, Somayazulu M, Mao Hk, Hemley RJ (2005), Crystal structure of the superconducting phases of S and Se *Physical Review B* 71:214104.
53. Clark SJ, Segall MD, Pickard CJ, Hasnip PJ, Probert MJ, Refson K, Payne MC (2005), First principles methods using CASTEP *Z Kristallogr* 220:567–570.
54. Kresse G, Furthmüller J (1996), Efficiency of ab initio total-energy calculations for metals and semiconductors using a plane-wave basis set *Comp Mat Sci* 6:15–50.
55. Baroni S, de Gironcoli S, Dal Corso A, Giannozzi P (2001), Phonons and related crystal properties from density-functional perturbation theory *Rev Mod Phys* 73:515–562.
56. Gonze X, Beuken JM, Caracas R, Detraux F, Fuchs M, Rignanese GM, Sindic L, Verstraete M, Zerah G, Jollet F, *et al.* (2002), First-principles computation of material properties: the ABINIT software project *Comp Mat Sci* 25:478–492.
57. Giannozzi P, Baroni S, Bonini N, Calandra M, Car R, Cavazzoni C, Ceresoli D, Chiarotti GL, Cococcioni M, Dabo I, *et al.* (2009), QUANTUM ESPRESSO: a modular and open-source software project for quantum simulations of materials *J Phys: Condens Matter* 21:395502.

Additional information The authors declare competing financial interests: details accompany the paper at [...]. Supplementary information accompanies this paper on [...].

Table 1. Structures of the newly predicted stable nitrogen phases. Q_M **is the Mulliken charge obtained from ultrasoft pseudopotential calculations, and** Q_B **is the Bader charge from PAW calculations.**

Structures	P (TPa)	lattice constants	atomic position	Q_M	Q_B
$Cmca$	2.5	a=2.090, b=3.041, c=2.617	8f (0.0, -0.6034, -0.1843)	0	0
		α=90, β=90, γ=90			
$P4/nbm$	2.5	a=3.424, b=3.424, c=2.466	2d (0.0, 0.5, 0.5)	0.18	-0.066
		α=90, β=90, γ=90	4g (0.0, 0.0, 0.7376)	0.11	0.183
			8m (0.1808, 0.6808, 0.7879)	-0.10	-0.075
$Fdd2$	8	a=5.715, b=4.590, c=2.404	16b (-0.8991, 0.9116, -0.8784)	-0.15	-0.359
		α=90, β=90, γ=90	16b (-0.7687, 0.6347, -0.7130)	0.14	0.379
			16b (-0.3059, 0.4036, -0.3075)	0.01	-0.020
$R\bar{3}m$	12	a=1.613, b=1.613, c=1.468	3b (0.0, 0.0, 0.5)	0	0
		α=90, β=90, γ=120			
$I4_1/amd$	30	a=0.890, b=0.890, c=3.452	4a (0.0, 0.25, 0.875)	0	0
		α=90, β=90, γ=90			

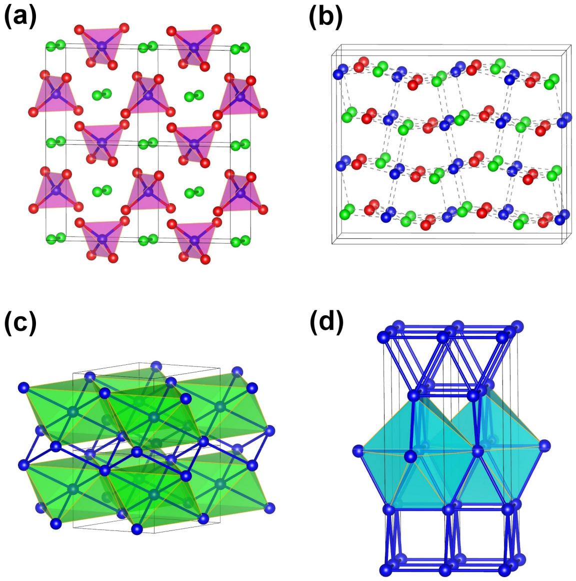

Fig. 1. Crystal structures of the newly predicted nitrogen phases. (a) $P4/nbm$, (b) $Fdd2$, (c) $R\bar{3}m$ and (d) $I4_1/amd$. The blue balls in (c) and (d) represent nitrogen atoms without obvious charge transfer. The colors in (a) and (b) represent atoms with different charges, see the text for more details. The tetrahedra in $P4/nbm$, octahedra in $R\bar{3}m$ and trigonal dodecahedron in $I4_1/amd$ are depicted in pink, green and cyan, respectively.

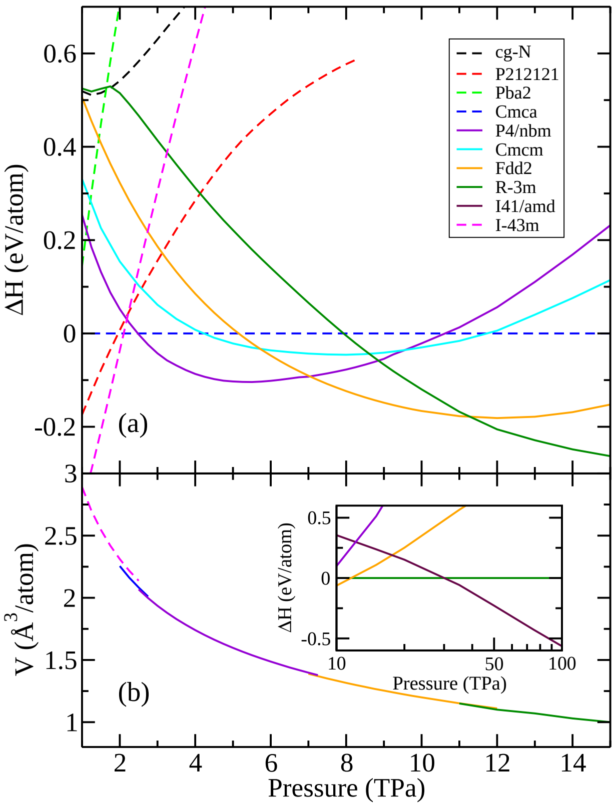

Fig. 2. (a) Enthalpy-pressure relations and (b) volumes. The enthalpies of the previously-reported polymeric phases are shown as dashed lines and the solid lines are new structures from this work. To make the plot clearer, only the volumes of the ground state structures are plotted in (b). The inset in (b) shows the enthalpies of $Fdd2$ and $I4_1/amd$ relative to $R\bar{3}m$ at very high pressures.

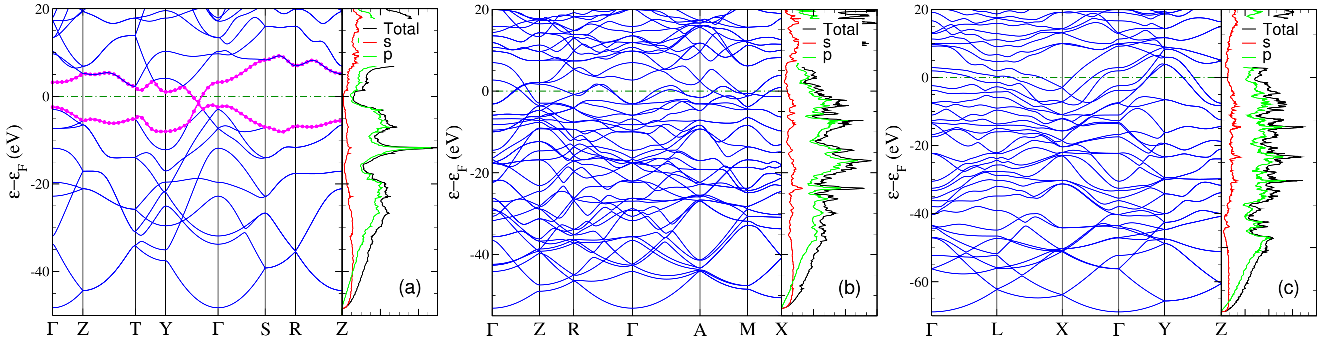

Fig. 3. Electronic band structures and projected densities of states (PDOS). (a) $Cmca$ at 2.0 TPa, (b) $P4/nbm$ at 3.0 TPa, (c) $Fdd2$ at 8.0 TPa. The zero of energy is at the Fermi level. The bands in $Cmca$ that form the partially filled Dirac cone are indicated by open circles.

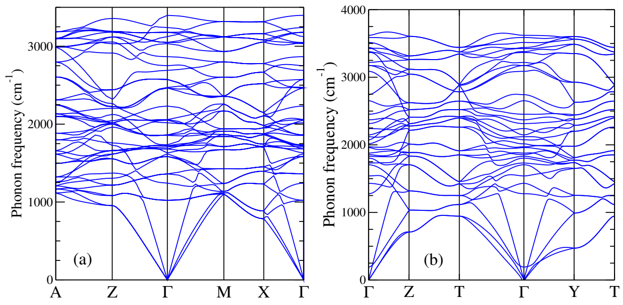

Fig. 4. Phonon dispersion relations. (a) $P4/nbm$ at 5 TPa, (b) $Fdd2$ at 8 TPa.

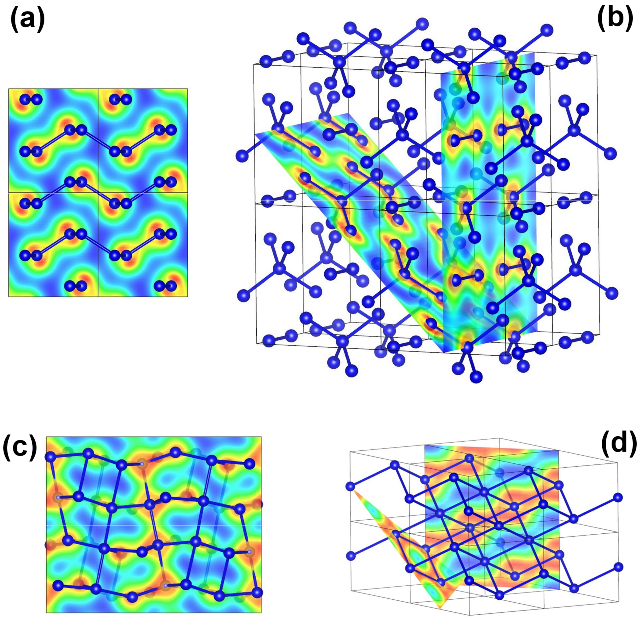

Fig. 5. Electron densities of polymeric nitrogen. (a) $Cmca$ at 2 TPa along [100] directions, (b) $P4/nbm$ at 2.5 TPa along [100] and [110] directions, (c) $Fdd2$ at 8 TPa along [001] directions. (d) $R\bar{3}m$ at 12 TPa along [110] and [$\bar{1}$11] directions.